Tandem Structure of Porous Silicon Film on Single-Walled Carbon Nanotube Macrofilms for Lithium-Ion Battery Applications

ARTICLE *in* ACS NANO · AUGUST 2010

Impact Factor: 12.88 · DOI: 10.1021/nn101196j · Source: PubMed

5 AUTHORS, INCLUDING:

Jiepeng Rong
University of Southern California
21 PUBLICATIONS **963** CITATIONS
SEE PROFILE

Jie Ni
Tsinghua University
10 PUBLICATIONS **195** CITATIONS
SEE PROFILE

Zhengjun Zhang
Tsinghua University
191 PUBLICATIONS **2,715** CITATIONS
SEE PROFILE

Bingqing Wei
University of Delaware
254 PUBLICATIONS **12,316** CITATIONS
SEE PROFILE

Tandem Structure of Porous Silicon Film on Single-Walled Carbon Nanotube Macrofilms for Lithium-Ion Battery Applications

Jiepeng Rong,[†] Charan Masarapu,[†] Jie Ni,[‡] Zhengjun Zhang,[‡] and Bingqing Wei[†,*]

[†]Department of Mechanical Engineering, University of Delaware, Newark, Delaware 19716 and [‡]Department of Materials Science and Engineering, Tsinghua University, Beijing 100084, People's Republic of China

ABSTRACT Development of materials and structures leading to high energy and power density lithium-ion batteries is a major challenge to the power needs of the electronic and automobile industries. Silicon is an attractive anode material being closely scrutinized for use in lithium-ion batteries but suffers from a poor cyclability and early capacity fading. In this work, we present a tandem structure of porous silicon film on single-walled carbon nanotube (SWNT) film to significantly improve the cycling stability of silicon as lithium-ion battery anode material. With this new structure configuration of the silicon films, a reversible specific capacity of 2221 mAh/g was retained after 40 charge—discharge cycles at 0.1 C rate, which is 3.6 times that of silicon film on a regular copper substrate and more than 11 times that of the SWNT film. The facile method is efficient and effective in improving specific capacity and stability of silicon anode lithium-ion batteries and will provide a powerful means for the development of lithium-ion batteries.

KEYWORDS: porous silicon · single-walled carbon nanotubes · tandem structure · lithium-ion battery · anode materials · electron beam evaporation

Electricity storage, the ability to capture and hold generated power during times of availability and retrieve it based on the need and demand, is a growing challenge among a broad range of renewable energy sources. Increasing efforts have been devoted to developing anode materials with a higher energy density and longer cycle life for lithium-ion batteries to meet the demands of the ever growing portable electronic and electric vehicle industries.[1−3] Silicon is an attractive anode material for lithium-ion batteries because it has a low discharge potential and the highest known theoretical charge capacity of 4200 mAh/g, 10 times higher than that of existing graphite anodes and other oxide and nitride materials.[4] However, its applications lag behind due to severe capacity fading caused by early pulverization that results in up to ~400% volumetric change during insertion and extraction of lithium ions.[5−7]

Thus far, it was evidenced that Si nanostructures, such as three-dimensional porous Si particles,[8] Si nanocomposites,[9] nestlike Si nanospheres,[10] Si nanotubes,[11] Si core−shell nanowires,[12] and amorphous or crystalline Si thin films,[13] have shown improved electrochemical performance over bulk Si material and are considered to be excellent candidates for high-performance electrode materials in lithium-ion batteries. Among the various Si nanostructures, filmlike Si nanostructures can provide additional advantages, for instance, compatibility with traditional battery design, good electric contact on current collectors, unnecessary binder material reduction, and more importantly, compatibility with modern semiconductor techniques for an easy scale-up.

However, studies have proved that the adherence of silicon films to current collectors is the key factor that governs the electrochemical performance of the lithium-ion batteries, and developing such kinds of anodes is very challenging.[14−16] Limited improvements have been reported on cycle stability and cycle life of lithium-ion batteries with Si thin films deposited on current collectors with modified surfaces by techniques, such as chemical etching or electroplating, but at the cost of either laborious pretreatment processes of substrates or decreasing specific energy density.[17,18]

In this work, we report a simple method to employ single-walled carbon nanotube (SWNT) macrofilms[19] as buffer layers between the Si thin films and the current collectors in order to significantly boost the electrochemical performance of the lithium-ion batteries. By simply coating a SWNT macrofilm on a regular copper current

*Address correspondence to weib@udel.edu.

Received for review May 28, 2010 and accepted July 20, 2010.

Published online July 23, 2010. 10.1021/nn101196j

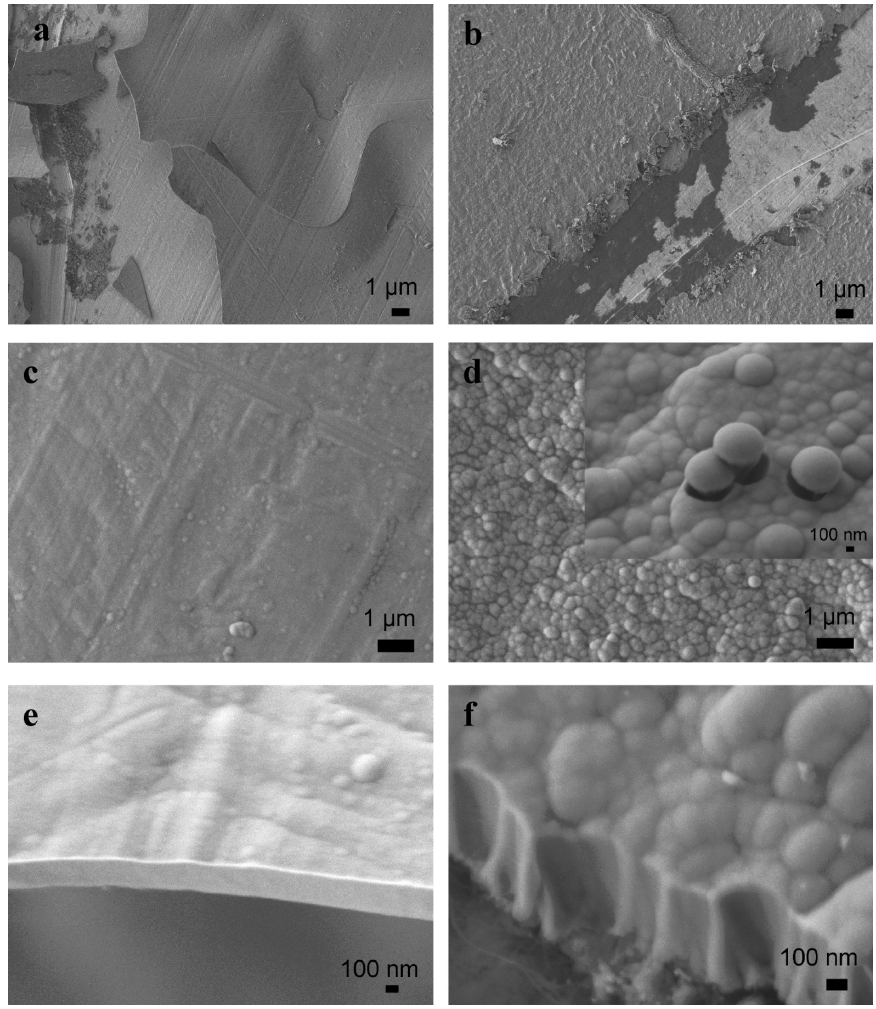

Figure 1. SEM images of as-prepared Si−Cu sample and Si−SWNT−Cu sample. (a,c,e) Top view and cross-section view of the Si−Cu sample are various magnifications separately; (b,d,f) Si−SWNT−Cu sample in corresponding manner. Inset of (d) shows clearly that some cone-shaped structures on Si−SWNT−Cu sample are squeezed out due to the internal stress induced during silicon deposition.

collector followed by physical deposition of a Si thin film to form a tandem structure, excellent electrochemical performance with a high reversible specific capacity has been achieved. The SWNT macrofilms not only provide excellent adhesion between the Si film, the SWNT film, and the copper substrate proved by SEM observations, galvanostatic charge−discharge cycling, and electrochemical impedance spectroscopy analysis but also are deformable and stretchable sample holders, which are able to tolerate the drastic volumetric expansion and shrinkage of Si films due to lithium-ion insertion and extraction. In addition, the SWNT macrofilm itself is a good candidate for anode material for lithium-ion batteries; it can easily be transferred to any substrate (such as copper foil) without damage to form extremely strong adhesion between the SWNT film and the current collector, which can withstand ultrasonication treatment. These unique advantages make this simple method attractive and practical for applications.

RESULTS AND DISCUSSION

Structures of As-Prepared Electrode Samples. Two kinds of substrates were used for electrode preparation in this study: one was bare copper foil (Cu) and the other was the copper foil coated with SWNT macrofilms, which function as buffer layers (SWNT−Cu). Detailed SWNT macrofilm preparation is presented in the Methods section. Silicon thin films were deposited on both substrates in a high-vacuum electron beam evaporation system under 8×10^{-5} Pa. To obtain the same thickness of silicon films on these two substrates, the bare Cu foil and SWNT-coated Cu foil were mounted on the substrate holder at the same time and with the same distance of 30 cm to the evaporation source, which is high-purity (99.999%) silicon target. The deposition rate (40 nm min^{-1}) and film thickness were controlled by a quartz crystal thickness monitor and a rate controller.

An immediate adhesion analysis of Si films on Cu and on SWNT−Cu substrates can be simply compared using the scratching method, as shown in Figure 1a,b. Under low magnification, we can see that cracks in the

silicon film inevitably formed. For those on the bare Cu substrate, cracks once formed spread quickly through a large area and make the whole film into small pieces, which lose attachment to the Cu foil substrate (Figure 1a). While cracks in silicon film on the SWNT−Cu foil are quite localized, the majority of the silicon film adheres fairly to the SWNT−Cu foil (Figure 1b). It is plausible that a strong internal stress could easily be formed during the physical deposition on the relatively smooth bare Cu surface. This can be further confirmed by top views of the samples under a higher magnification, where the silicon film on the Cu foil presents a relatively smooth and flat surface (Figure 1c). The silicon film on the SWNT−Cu substrate, however, has convex morphology with caps of cone-shaped "lattice" through the whole silicon film (Figure 1d). Some cones may be squeezed out to release the internal stress formed during the physical deposition (inset of Figure 1d). It is interesting to note that similar internal stress induced by lithium-ion insertion into silicon is also expected to facilitate some cone-shaped silicon "lattice" to be removed in order to provide free space for stress releasing, resulting in porous silicon film formation, which is proved by the experimental results.

This unique morphology is attributed to the uneven surface provided by the SWNT macrofilm. It has been recognized that a larger specific interface area would yield a better adhesion between two components.[20] The SWNT macrofilm, formed with tangled SWNT building blocks, provides a rough and large surface with nanosized features,[19] which enhance interface adhesion between the silicon film and the copper substrate. Meanwhile, the SWNT film facilitates the formation of the cone-shaped structures inside the Si film during physical deposition. These cone-shaped structures allow some "cone-caps" to be easily removed in order to release internal stress, benefiting electrochemical cycling stability as discussed below.

The microstructure difference is also reflected from the cross-section view of these two samples. The Si film on Cu foil exhibits a very smooth edge (Figure 1e) compared to a dental edge of the silicon film on SWNT−Cu foil (Figure 1f), which shows again cone-shaped grains. Both samples employed for electrochemical characterizations have the same thickness of ~300 nm (Figure 1e,f). XRD analysis (see Supporting Information) suggests an amorphous structure (a-Si) of the deposited silicon films, and no Si reflection peaks were detected except those from the copper substrate by XRD analysis.

Electrochemical Characteristics. Galvanostatic charge−discharge cycling stability measurements were carried out with three samples: 300 nm Si film on the bare Cu substrate (Si−Cu), 300 nm Si film on the SWNT film coated Cu substrate (Si−SWNT−Cu), and a pure SWNT film on the bare Cu (SWNT−Cu). For the first two samples, the charge−discharge cycling was conducted at 0.05 C rate for the first cycle and at 0.1 C rate for the subsequent cycles. The charge−discharge current rate was calculated based on the maximum theoretical capacity of silicon (*i.e.*, 4200 mAh/g). The third one (*i.e.*, the SWNT−Cu sample) was a control experiment which can provide information on the contribution portion from the SWNT film in the Si−SWNT−Cu electrode. Thus, the same current used for the first two samples was applied.

The charge−discharge experimental results (Figure 2) revealed that the battery cell with the Si−SWNT−Cu electrode showed the best electrochemical performance, in terms of both the specific capacity and the cycling stability compared to that with the Si−Cu electrode, which showed almost linear, sharp decrease during lithium-ion insertion and extraction (Figure 2a). First, second, and 41st charge−discharge voltage profiles of both Si−Cu (Figure 2c) and Si−SWNT−Cu (Figure 2d) reveal that, after 40 charge−discharge cycles, the specific discharge capacity of the Si−SWNT−Cu cell still retains 2221 mAh/g, which is about 3.6 times of the Si−Cu cell and 11.5 times the pure SWNT film cell. The Si−SWNT−Cu cell exhibited significantly improved capacity retention in comparison with the Si−Cu cell performance. After 40 charge−discharge cycles at 0.1 C rate, 82% of the specific discharge capacity is retained for the Si−SWNT−Cu cell, while only 42% percent is retained for the Si−Cu cell (Figure 2a).

To estimate the capacity contribution from the silicon film and from the SWNT film in the tandem structure configuration, the battery cell using the pure SWNT film as the anode electrode with the same weight as that in the Si−SWNT−Cu sample was characterized by applying the same current density. The cell consisting of the pure SWNT film gave 732, 288, and 193 mAh/g discharge capacity in the first, second, and 41st cycle (Figure 2a), which are 18.9, 10.6, and 8.7% of the discharge capacity of the Si−SWNT−Cu cell in the corresponding cycles, respectively, indicating that silicon dominated the capacity contribution in the Si−SWNT−Cu battery cell.

In addition, the tandem structure of the silicon film on the SWNT film shows a better Coulombic efficiency compared to the pure Si film and the pure SWNT film. The pure SWNT cell (SWNT−Cu) has about 44% first cycle Coulombic efficiency, indicating as high as more than 50% irreversibility. The Si film cell (Si−Cu) in this experiment shows 61% first cycle Coulombic efficiency, while the tandem structure cell (Si−SWNT−Cu) exhibits the highest first cycle Coulombic efficiency of ~74% (Figure 2b). The high Coulombic efficiency of the Si−SWNT−Cu cell may be associated with the tandem structure, where the silicon coating layer may decrease the occurrence of side reactions between the SWNT film and the electrolyte by reducing their direct contacts.

Compared to previous efforts to achieve larger gravimetric capacity, higher Coulumbic efficiency, and

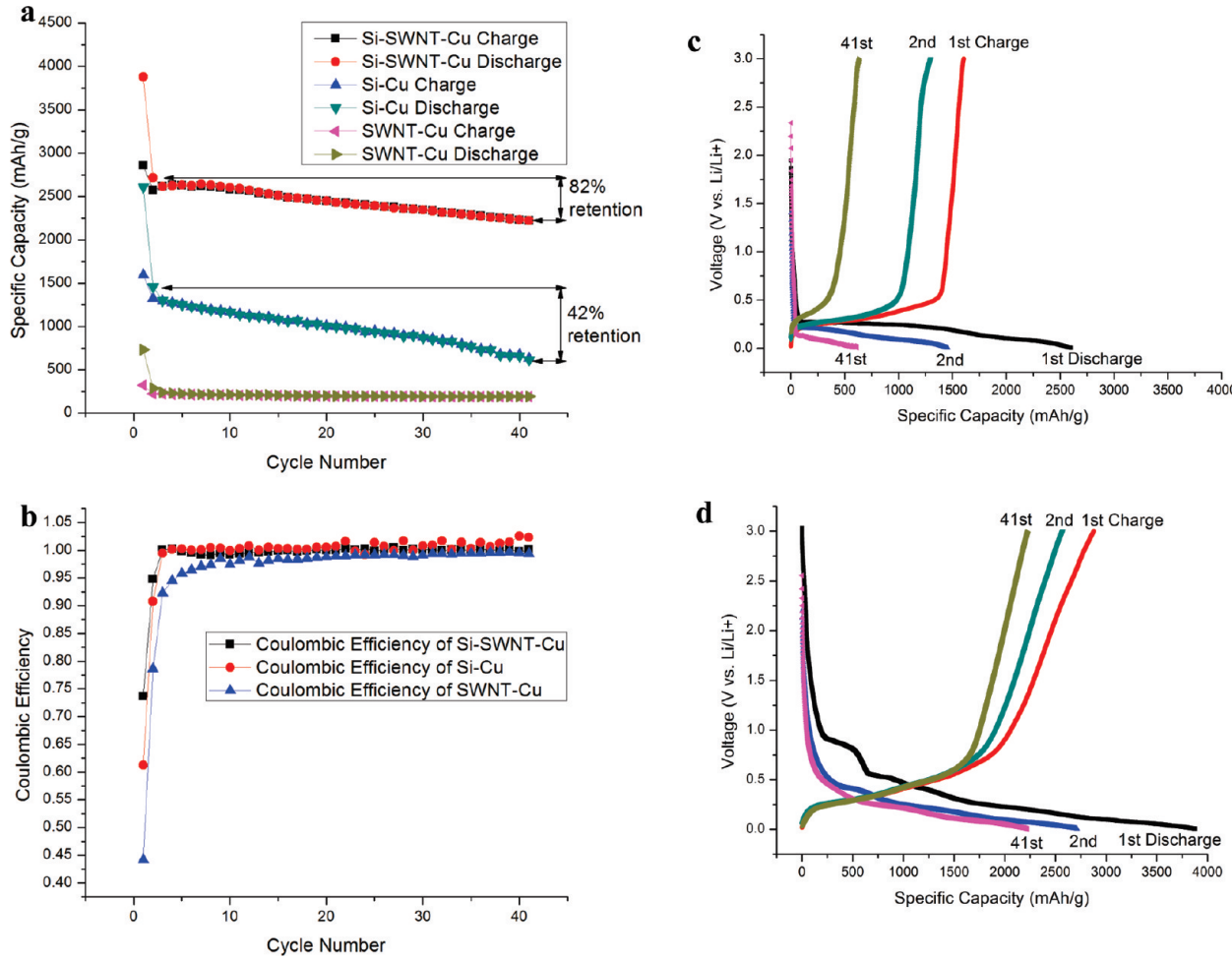

Figure 2. (a) Comparison of cycling performance of the batteries with Si−Cu, Si−SWNT−Cu, and SWNT−Cu samples as electrodes at constant current 0.05 C in the first cycle and 0.1 C in the remaining 40 cycles. (b) Comparison of Coulombic efficiency of these three electrodes. (c) Charge/discharge plots of first, second, and 41st cycles of Si−Cu. (d) Charge/discharge plots of first, second, and 41st cycles of Si−SWNT−Cu.

better cyclability on the usage of silicon as anode materials in lithium-ion batteries, which can be categorized as film-like Si anode,[13,18] Si composite anode,[9,21−23] and novel nanostructures of silicon anodes (such as nanoparticles, nanowires, nanotubes, nanorods, nest-like nanospheres, and three-dimensional porous particles),[8,10,11,24−26] our method either has a superior retention of specific capacity during long cycling or is facile and simple. For example, specific capacities of 800 mAh/g[18] and about 1000 mAh/g after 20 cycles[13] have been achieved using the film-like Si anodes; 500 to 1500 mAh/g has been observed after 20 cycles using the Si composite anodes.[9,21−23] With regard to the novel nanostructures of silicon, the third category mentioned above, 1000−1600 mAh/g stable capacity using nanorods,[24] nanowires,[25] and nanospheres,[10] has been observed after 40 charge−discharge cycles. Our experimental results show a better electrochemical performance in terms of both specific capacity and cycling stability. Thus far, better specific capacities with silicon nanowires, silicon nanotubes, and three-dimensional porous nanoparticles have been reported.[8,11,26] However, either chemical vapor deposition to synthesize silicon nanowire and nanotubes or sol−gel method and HF etching to form porous Si nanoparticles are much more laborious and time-consuming processes compared to this one-step silicon physical deposition.

Structural Analysis of Si Films after Continuous Cycling. After 40 charge−discharge cycles at 0.1 C rate, the battery cells were dissembled outside the glovebox and the electrodes were washed rigorously with ethanol for structural analysis. SEM observations of the Si−Cu electrode (Figure 3a,c) and the Si−SWNT−Cu electrode (Figure 3b,d) after cell dissembling revealed that the Si film on the bare Cu substrate was pulverized severely after cycling; only a small amount of silicon remained to connect to the Cu current collector as discontinuous particles with various sizes (Figure 3a,c). However, the silicon film was intact on the SWNT film after turning into porous structures. Although the silicon film broke into grain domains with gaps between them after lithiation/delithiation cycles, each grain domain maintained its strong adhesion onto the under laid continu-

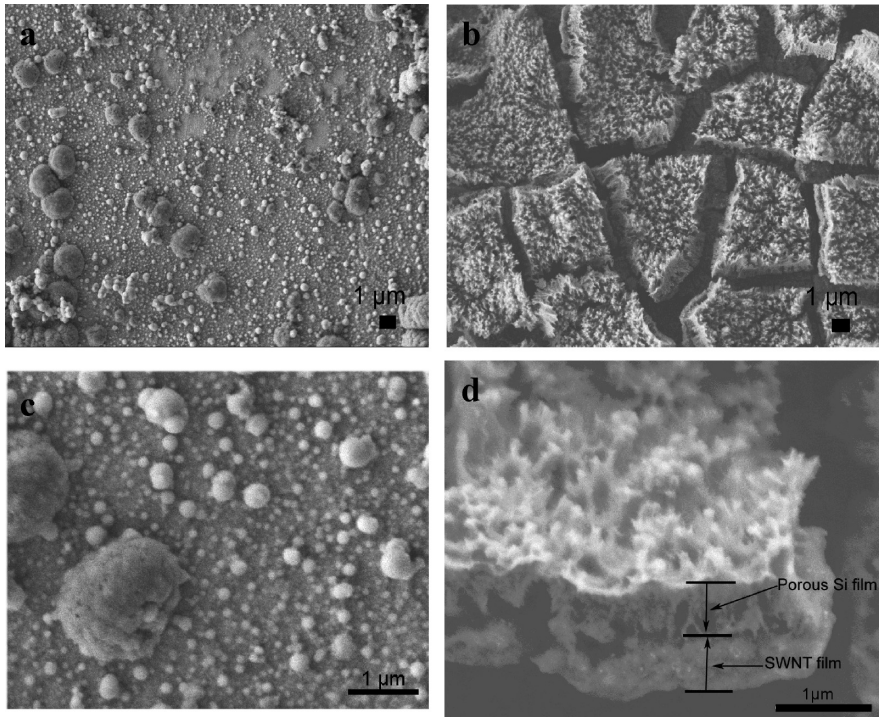

Figure 3. SEM images of Si−Cu electrodes and Si−SWNT−Cu electrodes after 40 cycles of charge−discharge at 0.1 C rate. (a,c) Si−Cu sample. Only minor discontinuous particles are left on the Cu substrate after cycling. (b,d) Si−SWNT−Cu sample. The majority of the silicon film is retained and keeps good contact on the Cu substrate through the SWNT film connections after rigorous washing. The uniform domains with porous structures are about 10 μm.

ous SWNT film (Figure 3b,d), even after rigorous washing. The excellent adhesion of the Si film can be attributed to the large specific surface area SWNT buffer layer, which is deformable, stretchable, and tolerant to the volumetric expansion and shrinkage of Si films due to lithium-ion insertion and extraction, compared to the smooth and rigid copper substrate (Figure 3a,c).

The structural evolution of silicon films upon charge−discharge cycling are illustrated in Scheme 1, where the left panel is for the Si−Cu electrode, fabri-

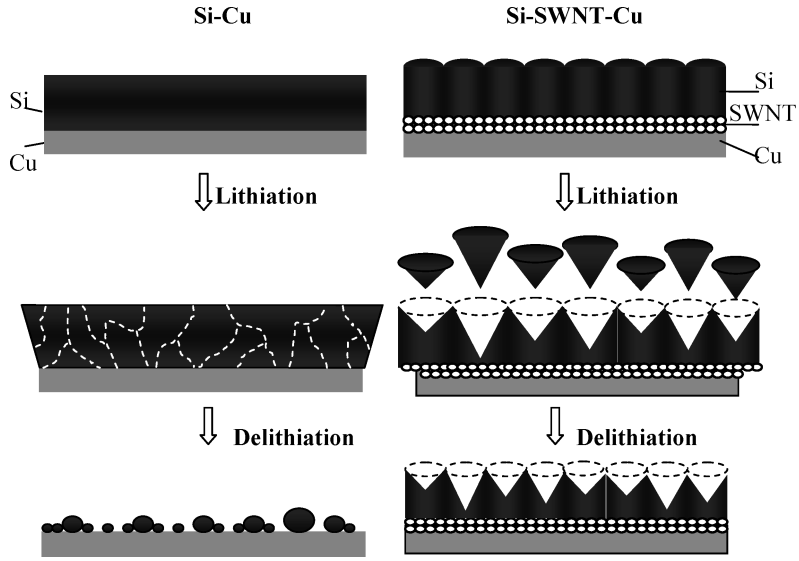

Scheme 1. Schematic representations (cross-section view) of structural evolution of silicon films upon charge−discharge cycling. Left panel is a Si−Cu sample, fabricated by physically depositing silicon film directly on a bare copper current collector; right panel represents a Si−SWNT−Cu sample with the SWNT macrofilm as a buffer layer between the deposited Si film and the copper current collector. After 40 charge−discharge cycles, the silicon film on the bare copper substrate pulverizes severely into discontinuous particles with various sizes and only a minority of the silicon particles remain on the current collector. The silicon film on the SWNT buffer layer becomes a porous structure but holds tightly onto the SWNT film after getting rid of a few cone-shaped silicon pieces. The structural difference of the Si film retention can be attributed to the large specific surface area SWNT buffer layer, which is deformable, stretchable, and tolerant to the volumetric expansion and shrinkage of Si films due to Li-ion insertion and extraction, compared to the smooth and rigid copper foil.

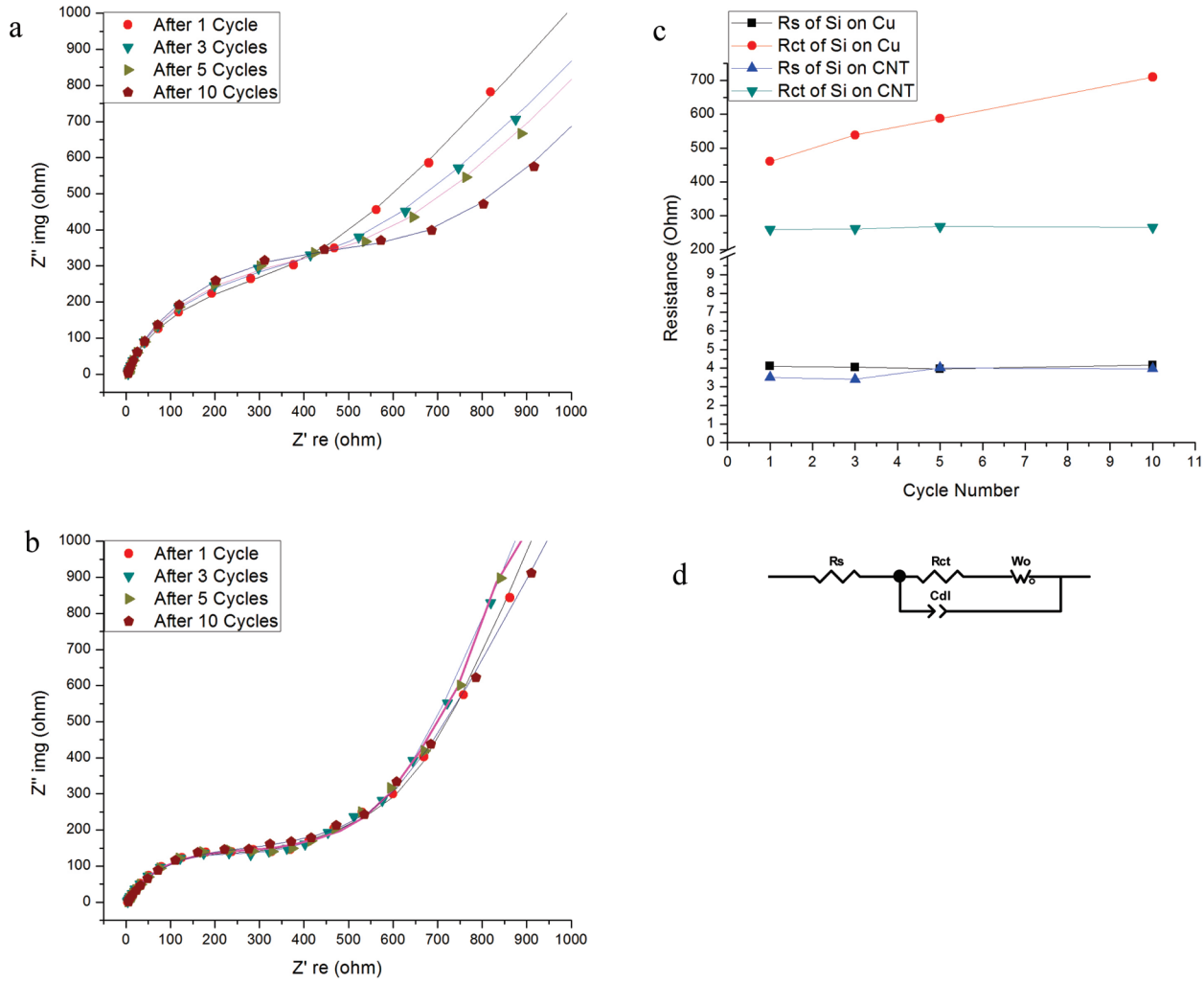

Figure 4. Electrochemical impedance spectroscopy measurements are performed on the cells with Si−Cu sample (a) and Si−SWNT−Cu sample (b) separately after the first, third, fifth, and 10th cycles. The dots in panels a and b are experimental data, and the lines are curve fitting data with corresponding equivalent circuit in panel d. Solution resistance (R_s) and charge transfer resistance (R_{ct}) of both Si−Cu and Si−SWNT−Cu samples are collected and plotted in panel c.

cated by physically depositing silicon film directly on a bare copper current collector, while the right panel represents the Si−SWNT−Cu electrode with the SWNT macrofilm as a buffer layer between the deposited Si film and the copper current collector. The silicon film on the bare copper substrate typically has a smooth, uniform, and dense layer structure, while the silicon film on the SWNT film coated substrate exhibits a column or cone-shaped "lattice" structure. During charge−discharge cycling, Si film on Cu experiences a significant volume expansion and pulverizes into discontinuous particles and only small amounts of silicon stay on the current collector after cycling. However, similar internal pressure in the Si−SWNT−Cu sample introduced by volumetric change during lithium-ion insertion/extraction can be released by getting rid of some cone-shaped silicon grains. The silicon film on the SWNT buffer layer, therefore, becomes a porous structure but holds tightly onto the SWNT film. The SWNT film provides deformable and stretchable tolerance to the volumetric expansion and shrinkage of the Si films due to lithium-ion insertion and extraction.

To further support the structural evolution model discussed above, electrochemical impedance analysis was conducted on all battery cells from 100 kHz to 10 mHz. The impedance of the anode in the lithium-ion batteries depends strongly on the lithium content inside the electrode materials. To maintain uniformity, electrochemical impedance spectroscopy measurements were carried out on the working electrodes at the delithiated state after the first, third, fifth, and 10th cycles, respectively. The Nyquist plots obtained are shown in Figure 4a,b, where the high frequency corresponds to the resistance of the electrolytes, R_s, the semicircle in the middle frequency range indicates the charge transfer resistance, R_{ct}, relating to the charge transfer through the electrode/electrolyte interface and the double layer capacity, C_{dl}, formed due to the electrostatic charge separation near the electrode/electrolyte interface. Also, the inclined line in the low frequency represents the Warburg impedance, W_o, which

is related to solid-state diffusion of lithium ions into the electrode material.

To evaluate effects of different impedance components on the cell degradation along cycling, the electrolyte resistance, R_s, and the charge transfer resistance, R_{ct}, were calculated and plotted in Figure 4c by fitting the Nyquist plots with the corresponding equivalent circuit based on Randles circuit (Figure 4d).[27] The electrolyte resistances of both samples are quite comparable within the monitored 10 cycles. However, the charge transfer resistance of the Si−Cu electrode increases significantly during cycling, indicating a larger electrochemical reaction resistance due to the electronic contact loss when the lithiation/delithiation processes take place. This resistance change explains well the rapid degradation of the specific capacity in the cell with the Si−Cu electrode. In contrast, stable charge transfer resistance is obtained for the Si−SWNT−Cu electrode during charge−discharge cycling, indicating an excellent structural stability of the electrode materials as well as a good electronic contact between the active materials and the current collector. These results from impedance analysis are in good agreement with the SEM observations and the charge−discharge cycling performance. As demonstrated in Figure 3b, the domain and porous structure formation released induced stress by losing small amounts of Si. However, this Si loss would not affect much the electrical contacts between the Si film and the SWNT film and between the SWNT film and the current collector. This is confirmed by the impedance analysis that the series resistance, R_s, and the charge transfer resistance, R_{ct}, are very stable with cycling, different from the Si−Cu sample in Figure 3a, where Si loses the contact with the current collector.

CONCLUSIONS

In summary, we present a simple method to fabricate tandem structure of porous silicon film on SWNT film to significantly improve the cycling stability of silicon film as a promising lithium-ion battery anode material. With the new structure using the SWNT film as a buffer layer, reversible specific capacity of silicon film retains 2221 mAh/g after 40 charge−discharge cycles at 0.1 C rate, which is more than 3 times the capacity of the silicon film on a bare copper current collector. The unique morphology and structure of the SWNT film not only provide enhanced adhesion between the silicon film and the current collector but also act as a deformable and stretchable substrate to be compliant with the volumetric expansion and shrinkage of the silicon film. The facile method and the tandem structure will provide a promising solution for the development of high density lithium-ion batteries.

METHODS

Preparation of SWNT Macrofilm. SWNT macrofilms were synthesized by a simple floating chemical vapor deposition (CVD) method using ferrocene as carbon feedstock/catalyst and sulfur as an additive to promote SWNT growth to a high percentage.[19] No additional carbon source is required. In detail, a solid volatile mixture of ferrocene and sulfur (atomic ratio Fe/S = 10:1) was introduced into a ceramic tube. CVD reaction took place at 1100−1150 °C under a gas flow of argon (1500 sccm) and hydrogen (150 sccm) mixture. After 10−30 min reaction, the furnace was allowed to cool to room temperature. The as-prepared SWNT macrofilms were purified by a combination of oxidation (heated at 450 °C in air for 1 h) and rinsing with acid (37% HCl) to remove amorphous carbon and catalytic iron nanoparticles. The SWNT macrofilms can be prepared to up to 200 cm^2 with our facility and can be easily transferred to any substrates without damage.

Preparation of Electrodes of Li-Ion Batteries. Cu foils used as electrode current collectors were coated with the SWNT macrofilms before Si thin film deposition. For comparison, bare Cu foil substrates were used as control samples. Both samples were punched with a standard arch puncher and accurately weighed before Si deposition. The electrodes of lithium-ion batteries for electrochemical testing in this study were weighed again after silicon deposition on different substrates. The mass weights from measurements are consistent with calculations from the Si deposition monitoring.

Characterizations. The as-prepared electrodes were structurally analyzed using scanning electron microscope (SEM) and X-ray diffraction techniques (XRD). Electrochemical performance was characterized by assembling two-electrode battery coin cells in an argon-filled glovebox with lithium metal as the reference and the counter electrode in 1 M $LiPF_6$ in EC/DEC electrolyte. Batteries with the Si−Cu anode and the Si−SWNT−Cu anode were characterized separately at 0.05 C in the first cycle and then 0.1 C rate for the subsequent 40 cycles within 3−0.005 V voltage range. For both samples, only silicon was considered as the active material for setting current density. The two samples have the same silicon weight, typically 0.15 mg due to same deposition parameters. After electrochemical measurements, the coin cells were dissembled outside the glovebox and washed with ethanol for SEM analysis.

Acknowledgment. We thank Dr. Lobo and G. Brett for help with XRD measurements. This work was supported by the National Science Foundation (CMMI0926093), Delaware NASA/EPSCoR RID Seed Grant (NNX07AT51A), and the Natural Science Foundation of China (NSFC No. 50828201).

Supporting Information Available: X-ray diffraction of the Si thin film deposited on Cu substrate. This material is available free of charge *via* the Internet at http://pubs.acs.org.

REFERENCES AND NOTES

1. Scrosati, B. Battery Technology—Challenge of Portable Power. *Nature* **1995**, *373*, 557–558.
2. Tarascon, J. M.; Armand, M. Issues and Challenges facing Rechargeable Lithium Batteries. *Nature* **2001**, *414*, 359–367.
3. Armand, M.; Tarascon, J. M. Building Better Batteries. *Nature* **2008**, *451*, 652–657.
4. Boukamp, B. A.; Lesh, G. C.; Huggins, R. A. All-Solid Lithium Electrodes with Mixed-Conductor Matrix. *J. Electrochem. Soc.* **1981**, *128*, 725–729.
5. Graetz, J.; Ahn, C. C.; Yazami, R.; Fultz, B. Highly Reversible Lithium Storage in Nanostructured Silicon. *Electrochem. Solid-State Lett.* **2003**, *6*, A194–A197.
6. Graetz, J.; Ahn, C. C.; Yazami, R.; Fultz, B. Nanocrystalline and Thin Film Germanium Electrodes with High Lithium Capacity and High Rate Capabilities. *J. Electrochem. Soc.* **2004**, *151*, A698–A702.

7. Maranchi, J. P.; Hepp, A. F.; Kumta, P. N. High Capacity, Reversible Silicon Thin-Film Anodes for Lithium-Ion Batteries. *Electrochem. Solid-State Lett.* **2003**, *6*, A198–A201.
8. Kim, H.; Han, B.; Choo, J.; Cho, J. Three-Dimensional Porous Silicon Particles for Use in High-Performance Lithium Secondary Batteries. *Angew. Chem., Int. Ed.* **2008**, *47*, 10151–10154.
9. Holzapfel, M.; Buqa, H.; Scheifele, W.; Novak, P.; Petrat, F.-M. A New Type of Nano-Sized Silicon/Carbon Composite Electrode for Reversible Lithium Insertion. *Chem. Commun.* **2005**, *12*, 1566–1568.
10. Ma, H.; Cheng, F. Y.; Chen, J.; Zhao, J. Z.; Li, C. S.; Tao, Z. L.; Liang, J. Nest-like Silicon Nanospheres for High-Capacity Lithium Storage. *Adv. Mater.* **2007**, *19*, 4067.
11. Park, M. H.; Kim, M. G.; Joo, J.; Kim, K.; Kim, J.; Ahn, S.; Cui, Y.; Cho, J. Silicon Nanotube Battery Anodes. *Nano Lett.* **2009**, *9*, 3844–3847.
12. Cui, L. F.; Yang, Y.; Hsu, C. M.; Cui, Y. Carbon−Silicon Core−Shell Nanowires as High Capacity Electrode for Lithium Ion Batteries. *Nano Lett.* **2009**, *9*, 3370–3374.
13. Zhang, T.; Zhang, H. P.; Yang, L. C.; Wang, B.; Wu, Y. P.; Takamura, T. The Structural Evolution and Lithiation Behavior of Vacuum-Deposited Si Film with High Reversible Capacity. *Electrochim. Acta* **2008**, *53*, 5660–5664.
14. Beaulieu, L. Y.; Eberman, K. W.; Turner, R. L.; Krause, L. J.; Dahn, J. R. Colossal Reversible Volume Changes in Lithium Alloys. *Electrochem. Solid-State Lett.* **2001**, *4*, A137–A140.
15. Park, M. S.; Wang, G. X.; Liu, H. K.; Dou, S. X. Electrochemical Properties of Si Thin Film Prepared by Pulsed Laser Deposition for Lithium Ion Micro-batteries. *Electrochim. Acta* **2006**, *51*, 5246–5249.
16. Moon, T.; Kim, C.; Park, B. Electrochemical Performance of Amorphous-Silicon Thin Films for Lithium Rechargeable Batteries. *J. Power Sources* **2006**, *155*, 391–394.
17. Yin, J. T.; Wada, M.; Yamamoto, K.; Kitano, Y.; Tanase, S.; Sakai, T. Micrometer-Scale Amorphous Si Thin-Film Electrodes Fabricated by Electron-Beam Deposition for Li-Ion Batteries. *J. Electrochem. Soc.* **2006**, *153*, A472–A477.
18. Kim, Y. L.; Sun, Y. K.; Lee, S. M. Enhanced Electrochemical Performance of Silicon-Based Anode Material by Using Current Collector with Modified Surface Morphology. *Electrochim. Acta* **2008**, *53*, 4500–4504.
19. Zhu, H. W.; Wei, B. Q. Direct Fabrication of Single-Walled Carbon Nanotube Macro-films on Flexible Substrates. *Chem. Commun.* **2007**, *29*, 3042–3044.
20. Kinloch, A. J. The Science of Adhesion 1. Surface and Interfacial Aspects. *J. Mater. Sci.* **1980**, *15*, 2141–2166.
21. Wilson, A. M.; Dahn, J. R. Lithium Insertion in Carbons Containing Nanodispersed Silicon. *J. Electrochem. Soc.* **1995**, *142*, 326–332.
22. Ng, S. H.; Wang, J. Z.; Wexler, D.; Konstantinov, K.; Guo, Z. P.; Liu, H. K. Highly Reversible Lithium Storage in Spheroidal Carbon-Coated Silicon Nanocomposites as Anodes for Lithium-Ion Batteries. *Angew. Chem., Int. Ed.* **2006**, *45*, 6896–6899.
23. Liu, Y.; Wen, Z. Y.; Wang, X. Y.; Yang, X. L.; Hirano, A.; Imanishi, N.; Takeda, Y. Improvement of Cycling Stability of Si Anode by Mechanochemcial Reduction and Carbon Coating. *J. Power Sources* **2009**, *189*, 480–484.
24. Teki, R.; Datta, M. K.; Krishnan, R. T.; Parker, C.; Lu, T. M.; Kumta, P. N.; Koratkar, N. Nanostructured Silicon Anodes for Lithium Ion Rechargeable Batteries. *Small* **2009**, *5*, 2236–2242.
25. Laik, B.; Eude, L.; Pereira-Ramos, J. P.; Cojocaru, C. S.; Pribat, D.; Rouviere, E. Silicon Nanowires as Negative Electrode for Lithium-Ion Microbatteries. *Electrochim. Acta* **2008**, *53*, 5528–5532.
26. Chan, C. K.; Peng, H. L.; Liu, G.; McIlwrath, K.; Zhang, X. F.; Huggins, R. A.; Cui, Y. High-Performance Lithium Battery Anodes Using Silicon Nanowires. *Nat. Nanotechnol.* **2008**, *3*, 31–35.
27. Randles, J. E. B. Kinetics of Rapid Electrode Reactions. *Discuss. Faraday Soc.* **1947**, *1*, 11–19.